Solid-State Electronics Vol. 22, pp. 241–248

0038-1101/79/0301-0241/$02.00/0

CARRIER TRANSPORT ACROSS HETEROJUNCTION INTERFACES†

C. M. WU and E. S. YANG

Department of Electrical Engineering and Computer Science, Columbia University, New York, NY 10027, U.S.A.

(*Received date* 30 *May* 1978; *in revised form* 4 *August* 1978)

Abstract—A general theory is presented to describe the carrier transport across heterojunction interfaces. In matching the boundary conditions at the interface, the conservation of total energy and perpendicular momentum is assumed and the difference of effective masses on two sides of the junction is taken into account. The quantum mechanical transmission coefficient is calculated by a combined numerical and WKB method. Application of the present model to an $Al_xGa_{1-x}As$–GaAs N-n heterojunction is performed and it gives rise to rectifying characteristics together with non-saturated reverse current. Comparison with the classical thermionic emission model is made to show the significance of tunneling and effect of quantum mechanical reflection.

1. INTRODUCTION

In the early semiconductor literature, the continuity and transport equations along with the Poisson's equation have been employed to describe the electrical characteristics of semiconductor devices. Shockley[1] and Schottky[2] developed the diffusion models for the p-n junction and the metal-semiconductor junction, respectively, under the assumption of constant quasi-Fermi level. The thermionic-emission theory of the Schottky barrier was presented by Bethe[3] who considered the current contributed by carriers with a kinetic energy greater than the barrier height. The importance of tunneling through a barrier was later described by Kane[4] and Harrison[5] in which the quantum mechanical transmission probability of carriers was introduced. The theory of field emission was presented by Stratton[6] who extended the theory of thermionic emission to include tunneling and took into account the deviation of the effective mass from the free electron mass. Significant contribution to the Schottky barrier theory was made by Crowell and Sze[7, 8] who also calculated the quantum mechanical transmission coefficient (QMT) of carriers passing through the interface[9].

Current conduction in heterojunctions was first investigated by Anderson[10] who made use of Shockley and Bethe's models. The Anderson model was extended by various investigators[11–16] who employed the thermionic, tunneling and diffusion models derived for the homojunction and the Schottky barrier. It should be pointed out that the assumptions in deriving the models in p-n homojunction and Schottky barrier do not necessarily apply to the heterojunction, particularly under the conditions that the difference between effective masses on the two sides of the junction is large, that the thermionic field emission is significant and that carrier accumulation exists at the interface. Summaries of the transport theory are given by Milnes and Feucht[17] and by Casey and Panish[18].

†Work supported by JSEP Contract DAAG29-77-C-0019 and by National Science Foundation.

The p-n homojunction and the Schottky barrier may be considered as two forms of the semiconductor heterojunction[19]. The homojunction is a special anisotype heterojunction with the same semiconductor on both sides of the junction. The Schottky barrier is a special isotype heterojunction with a strongly degenerate material, i.e. metal, on one side and the semiconductor on the other side. Thus, a generalized transport theory can be written using the heterojunction as the basic structure for calculation. This paper presents such a model, covering mechanisms of thermionic emission and tunneling. The significance of the QMT is explained and numerical calculation is used in the region where the WKB method is not applicable. The importance of the effective mass difference is elucidated. The two-dimensional effect in momentum space is accounted by making use of the conservation of total energy and perpendicular momentum. Calculated results of an $Al_xGa_{1-x}As$–GaAs N-n isojunction are presented.

2. CARRIER TRANSPORT ACROSS A POTENTIAL BARRIER OF HETEROJUNCTION

The transport of carriers from one side of the heterojunction to the other is characterized by the quantum-mechanical transmission coefficient (QMT), defined as the ratio of the transmitted to the incident current. The current per unit area from side 1 to side 2 of the junction in the x-direction is given by

$$J_{1\to 2}=\frac{2q}{(2\pi)^3}\int\int\int\frac{1}{\hbar}\left(\frac{\partial E}{\partial k_x}\right)\mathrm{d}k_x\,\mathrm{d}k_y\,\mathrm{d}k_z T(E,k_y,k_z)f_1(E(\bar{k}))\{1-f_2(E(\bar{k}))\} \quad (1)$$

where k_x, k_y and k_z are the wave vectors in the x, y and z directions respectively. Since heterojunctions used in optical devices are mostly fabricated with the direct-band semiconductor, we assume that the electron effective mass m^* is isotropic. In addition,

$T(E, k_y, k_z)$ = the quantum mechanical transmission coefficient of the carrier across the junction

E = the kinetic energy of the carrier

$$= \frac{\hbar^2}{2m^*}\bar{k}^2$$

$$= \frac{\hbar^2}{2m^*}(k_x^2 + k_y^2 + k_z^2)$$

f_1, f_2 = the probability of the carrier occupancy at the energy E in side 1 and side 2, respectively.

Here, electrons are considered as the only carriers and the formulae are valid for holes. Then the net current is the difference of the two current components flowing in opposite directions,

$$J = J_{1\to 2} - J_{2\to 1}$$

$$= \frac{2q}{(2\pi)^3}\int\int\int \frac{1}{\hbar}\left(\frac{\partial E}{\partial k_x}\right) dk_x\, dk_y\, dk_z T(E, k_y, k_z) \times \{f_1(E(\bar{k})) - f_2(E(\bar{k}))\}. \quad (2)$$

Equation (2) can be rewritten as

$$J = J_1 - J_2 \quad (3)$$

and

$$J_1 = \frac{2q}{(2\pi)^3}\int\int\int \frac{1}{\hbar}\left(\frac{\partial E}{\partial k_x}\right) dk_x\, dk_y\, dk_z T(E, k_y, k_z) f_1(E(\bar{k}))$$

$$= \frac{m^* q}{2\pi^2\hbar^3}\int dE_\parallel \int dE_\perp T(E_\parallel, E_\perp) f_1(E_\parallel, E_\perp) \quad (4)$$

where J_1 is the emission current from side 1 to side 2. A similar equation for J_2 can be obtained by interchanging the subscripts 1 and 2. The following relations have been used in obtaining eqn (4)

$$E_\perp = \frac{\hbar^2}{2m^*}(k_y^2 + k_z^2)$$

$$E_\parallel = \frac{\hbar^2 k_x^2}{2m^*},$$

where $E_\parallel$ is the kinetic energy along the current direction and $E_\perp$ is the kinetic energy perpendicular to the current direction. J_1 can be written in terms of the normalized kinetic energies,

$$J_1 = \frac{qm^* k^2 T^2}{2\pi^2\hbar^3}\int d\tilde{E}_\parallel \int d\tilde{E}_\perp T(\tilde{E}_\parallel, \tilde{E}_\perp) f_1(\tilde{E}_\parallel, \tilde{E}_\perp)$$

$$= A^* T^2 \int d\tilde{E}_\parallel \int d\tilde{E}_\perp T(\tilde{E}_\parallel, \tilde{E}_\perp) f_1(\tilde{E}_\parallel, \tilde{E}_\perp) \quad (5)$$

where $\tilde{E}_\parallel = E_\parallel/kT$, $\tilde{E}_\perp = E_\perp/kT$, A^* = the Richardson's constant of the semiconductor in side 1, k = Boltzmann's constant.

It is found that J_1 and J_2 have the same form except for the carrier occupancy probability f_1 and f_2. Although J_2 is expressed in terms of the material parameters of side 1, we can reformulate it as an invariant form in terms of material parameters of side 2 by keeping the transition matrix not vanished. In that case, the upper and lower bounds of the integral will be limited, and the total energy and perpendicular momentum are conserved during the transition. Figure 1 shows an arbitrary-shaped barrier, and the electron is incident from side 1 to side 2, or vice verse. Then, the conservation of energy and perpendicular momentum yields

$$E = E_\perp + E_\parallel = E'_\perp + E'_\parallel + E_B \quad (6)$$

$$m^* E_\perp = m^{*\prime} E'_\perp \quad (7)$$

or

$$\tilde{E}'_\perp = \frac{1}{\vartheta}\tilde{E}_\perp \quad (8)$$

$$\tilde{E}'_\parallel = \tilde{E}_\parallel + \left(1 + \frac{1}{\vartheta}\right)\tilde{E}_\perp - \tilde{E}_B \quad (9)$$

where $\vartheta = m^{*\prime}/m^*$ and the primed notation are the parameters of side 2. Since $\tilde{E}_\perp$, $\tilde{E}'_\perp$, $\tilde{E}_\parallel$ and $\tilde{E}'_\parallel$ are all required to be positive, the upper and lower bounds of the integral can be determined and J_1 and J_2 are given by

$$J_1 = A^* T^2 \int_{\max(\tilde{E}_B, 0)}^{\infty} d\tilde{E}_\parallel \int_0^{(\tilde{E}_\parallel - \tilde{E}_B)/(1/\vartheta - 1)} \times d\tilde{E}_\perp T(\tilde{E}_\parallel, \tilde{E}_\perp) f_1(\tilde{E}_\parallel, \tilde{E}_\perp); \quad \text{if } \vartheta < 1 \quad (10)$$

$$= A^* T^2 \int_0^{\infty} d\tilde{E}_\parallel \int_{\max[(\tilde{E}_B - \tilde{E}_\parallel)/(1 - 1/\vartheta), 0]}^{\infty} \times d\tilde{E}_\perp T(\tilde{E}_\parallel, \tilde{E}_\perp) f_1(\tilde{E}_\parallel, \tilde{E}_\perp); \quad \text{if } \vartheta > 1 \quad (11)$$

where $A^* = (qm^* k^2/2\pi^2\hbar^3)$

and $f_1(\tilde{E}_\parallel, \tilde{E}_\perp) = [1 + \exp(-\tilde{E}_{fn1} + \tilde{E}_\perp + \tilde{E}_\parallel)]^{-1}$

$$J_2 = A^* T^2 \int_{\max(\tilde{E}_B, 0)}^{\infty} d\tilde{E}_\parallel \int_0^{(\tilde{E}_\parallel - \tilde{E}_B)/(1/\vartheta - 1)} \times d\tilde{E}_\perp T(\tilde{E}_\parallel, \tilde{E}_\perp) f_2(\tilde{E}_\parallel, \tilde{E}_\perp)$$

$$= A^{*\prime} T^2 \int_0^{\infty} d\tilde{E}'_\parallel \int_{\max[(-\tilde{E}_B - \tilde{E}'_\parallel)/(1 - \vartheta), 0]}^{\infty} \times d\tilde{E}'_\perp T(\tilde{E}'_\parallel, \tilde{E}'_\perp) f_2(\tilde{E}'_\parallel, \tilde{E}'_\perp); \quad \text{if } \vartheta < 1 \quad (12)$$

$$= A^* T^2 \int_0^{\infty} d\tilde{E}_\parallel \int_{\max[(\tilde{E}_B - \tilde{E}_\parallel)/(1 - 1/\vartheta), 0]}^{\infty} \times d\tilde{E}_\perp T(\tilde{E}_\parallel, \tilde{E}_\perp) f_2(\tilde{E}_\parallel, \tilde{E}_\perp)$$

$$= A^{*\prime} T^2 \int_{\max(-\tilde{E}_B, 0)}^{\infty} d\tilde{E}'_\parallel \int_0^{(\tilde{E}'_\parallel + \tilde{E}_B)/(\vartheta - 1)} \times d\tilde{E}'_\perp T(\tilde{E}'_\parallel, \tilde{E}'_\perp) f_2(\tilde{E}'_\parallel, \tilde{E}'_\perp); \quad \text{if } \vartheta > 1 \quad (13)$$

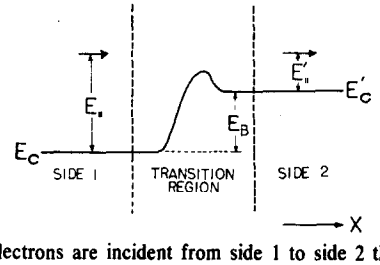

Fig. 1. Electrons are incident from side 1 to side 2 through an arbitrary-shape barrier.

where $A^{*\prime} = (qm^{*\prime}k^2/2\pi^2\hbar^3)$

$$f_2(\tilde{E}_\parallel, \tilde{E}_\perp') = [1+\exp(-\tilde{E}_{fn2}+\tilde{E}_\perp'+\tilde{E}_\parallel)]^{-1}$$
$$= [1+\exp(-\tilde{E}_{fn1}+\tilde{E}_\perp+\tilde{E}_\parallel+\tilde{V}_{BS})]^{-1}$$
$$\tilde{V}_{BS} = \tilde{E}_{fn1}-\tilde{E}_{fn2}-\tilde{E}_B.$$

$\tilde{V}_{BS}$ is the normalized bias voltage across the junction with the positive polarity on side 2. Therefore, both J_1 and J_2 can be expressed in the form of the emission current identical to that of emission from the semiconductor to the vacuum. However, the QMT here denotes the probability of carrier transmission from one semiconductor to another semiconductor. If the semiconductors are not degenerate, the Boltzmann's distribution can be used to simplify J_1 and J_2

$$J_1 = A^*T^2\exp(\tilde{E}_{fn1})$$
$$\times\int d\tilde{E}_\parallel \exp(-\tilde{E}_\parallel)\int d\tilde{E}_\perp T(\tilde{E}_\parallel,\tilde{E}_\perp)\exp(-\tilde{E}_\perp)$$
$$= A^*T^2\eta_1\exp(\tilde{E}_{fn1}) \quad (14)$$

and

$$J_2 = A^*T^2\exp(\tilde{E}_{fn2}+\tilde{E}_B)$$
$$\times\int d\tilde{E}_\parallel \exp(-\tilde{E}_\parallel)\int d\tilde{E}_\perp T(\tilde{E}_\parallel,\tilde{E}_\perp)\exp(-\tilde{E}_\perp)$$
$$= A^*T^2\eta_1\exp(\tilde{E}_{fn1})\exp(-\tilde{V}_{BS}) \quad (15)$$

where

$$\eta_1 = \int_{\max(\tilde{E}_B,0)}^{\infty} d\tilde{E}_\parallel \exp(-\tilde{E}_\parallel)\int_0^{(\tilde{E}_\parallel-\tilde{E}_B)/(1/\vartheta-1)} \times d\tilde{E}_\perp T(\tilde{E}_\parallel,\tilde{E}_\perp)\exp(-\tilde{E}_\perp); \quad \text{if } \vartheta<1 \quad (16)$$

$$= \int_0^{\infty} d\tilde{E}_\parallel \exp(-\tilde{E}_\parallel)\int_{\max[(\tilde{E}_B-\tilde{E}_\parallel)/(1-1/\vartheta),0]} \times d\tilde{E}_\perp T(\tilde{E}_\parallel,\tilde{E}_\perp)\exp(-\tilde{E}_\perp); \quad \text{if } \vartheta>1. \quad (17)$$

The integration limits in eqns (14) and (15) are the same as those in eqns (10)–(13). Therefore, the net current across the junction will be

$$J = A^*T^2\eta_1\exp(\tilde{E}_{fn1})[1-\exp(-\tilde{V}_{BS})]. \quad (18)$$

Similarly, J can be written in terms of the parameters of side 2 and is given by

$$J = A^{*\prime}T^2\eta_2\exp(\tilde{E}_{fn2})[\exp(\tilde{V}_{BS})-1] \quad (19)$$

where

$$\eta_2 = \int_0^{\infty} d\tilde{E}_\parallel' \exp(-\tilde{E}_\parallel')\int_{\max[(-\tilde{E}_B-\tilde{E}_\parallel')/(1-\vartheta),0]}^{\infty} \times d\tilde{E}_\perp' T(\tilde{E}_\parallel',\tilde{E}_\perp')\exp(-\tilde{E}_\perp'); \quad \text{if } \vartheta<1 \quad (20)$$

$$= \int_{\max(-\tilde{E}_B,0)}^{\infty} d\tilde{E}_\parallel' \exp(-\tilde{E}_\parallel')\int_0^{(\tilde{E}_\parallel'+\tilde{E}_B)/(\vartheta-1)} \times d\tilde{E}_\perp' T(\tilde{E}_\parallel',\tilde{E}_\perp')\exp(-\tilde{E}_\perp'); \quad \text{if } \vartheta>1. \quad (21)$$

Here, η's are defined to express the current density in terms of the thermal current $A^*T^2\exp(\tilde{E}_{fn})$ of the bulk material. They can be seen as a modification factor to the thermal current which depends upon the band bending of junction. The modification factor is dependent on the minority carrier life-time in the event the junction current is dominated by the diffusion mechanism. This case, however, is not discussed here. From eqns (16), (17), (20) and (21), we get

$$\eta_2 = \vartheta\eta_1\exp(\tilde{E}_B). \quad (22)$$

Either η_1 or η_2 can be used to express the current under the bias V_{BS}, but η_1 is usually appropriate as the current is saturated at the thermal current and η_2 is used to express the low voltage case with the customary exponential form. Both η_1 and η_2 are strongly dependent on the QMT. In the next section the cases of the ideal step-function barrier and N-n junction will be calculated and discussed.

3. CALCULATION OF THE QUANTUM MECHANICAL TRANSMISSION COEFFICIENT (QMT)

The QMT is defined as the ratio of the transmitted current to the incident, i.e. the probability of a carrier passing through a junction interface. From Crowell's analysis, the QMT of the depletion region of a Schottky barrier depends on the potential height and the material parameter[20] $E_{oo} = 1.8565\times10^{-11}(N/m_r\epsilon_r)^{1/2}$. The WKB approximation is valid when the carrier's kinetic energy is not near the peak of the potential. In the Schottky diode, electrons are emitted to a region with a larger effective mass, (the free electron mass); therefore, the current transport is very sensitive to the value of the effective mass ratio ϑ. In the heterojunction, the carrier transport through the junction is affected by the change of the effective mass which makes the perpendicular kinetic energy to be added or substracted depending on the value of ϑ. An ideal step-function barrier is first used in the following paragraphs to explain the effect of the conservation of the perpendicular momentum with different values of ϑ. Following the consideration of this idealized model, the carrier transport through a heterojunction is calculated.

(a) *Ideal step-function barrier*

With the boundary conditions that the Bloch wave function ψ is continuous through the junction interface $x = 0$,

$$\psi(0+) = \psi(0-) \quad (23)$$

and its derivative is modulated with a factor ϑ,

$$\left.\frac{d\psi}{dx}\right|_{x=0+} = \vartheta\left.\frac{d\psi}{dx}\right|_{x=0-} \quad (24)$$

the QMT of the ideal step-function barrier shown in Fig. 2 is

$$T(k_1,k_2) = \frac{4\vartheta k_1k_2}{(\vartheta k_1+k_2)^2} \quad (25)$$

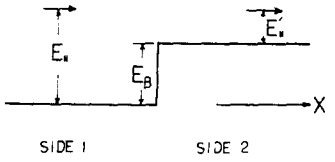

Fig. 2. Electrons are incident from side 1 to side 2 through an ideal step-function barrier.

where k_1, k_2 = the parallel momentum in side 1 and side 2, respectively. Equation (25) can be rewritten in terms of the kinetic energy of side 1,

$$T(E_\parallel, E_\perp) = \frac{4\sqrt{(\vartheta E_\parallel)}\sqrt{(E_\parallel + (1-1/\vartheta)E_\perp - E_B)}}{[\sqrt{(\vartheta E_\parallel)} + \sqrt{(E_\parallel + (1-1/\vartheta)E_\perp - E_B)}]^2}. \tag{26}$$

When ϑ is not equal to one, we can find that the change of the kinetic energy due to the transport effectively increases or decreases the barrier height. The magnitude of this effective barrier height depends on the value of ϑ. When ϑ is equal to one, the QMT will be reduced to a simple form which is independent of the perpendicular kinetic energy,

$$T(E_\parallel) = \frac{4\sqrt{(E_\parallel)}\sqrt{(E_\parallel - E_B)}}{[\sqrt{(E_\parallel)} + \sqrt{(E_\parallel - E_B)}]^2}. \tag{27}$$

The probability of the carrier occupancy obeys Boltzmann's distribution as the semiconductor is non-degenerate. Since the QMT's of carriers transporting in the opposite directions are the same, we only consider the case $\vartheta < 1$ and substitute eqn (26) in eqn (16). By the numerical integration, η_1 is calculated as a function of the barrier height of both positive and negative value. The different values of the mass ratio ϑ is also considered and their effects are shown in Fig. 3 and Fig. 4. In Fig. 3, η_1 is modified by the exponential of the normalized barrier height $\tilde{E}_B$ to show the effect of the reduction of the QMT due to the barrier height. This modified value is given by

$$\tilde{\eta} = \eta_1 \exp(\tilde{E}_{B0}) \tag{28}$$

where $\tilde{E}_{B0} = \max(\tilde{E}_B, 0)$. When $\tilde{E}_B$ increases positively, $\tilde{\eta}$ becomes small because the QMT decreases. If $\tilde{E}_B$ is less than zero, the increase of the magnitude of $\tilde{E}_B$ will

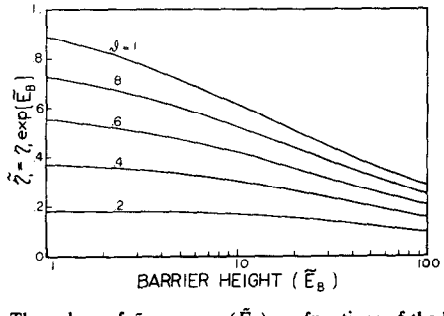

Fig. 3. The values of $\tilde{\eta}_1 = \eta_1 \exp(\tilde{E}_B)$ are functions of the barrier with the effective mass ratio ϑ. $\tilde{E}_B = E_B/kT$.

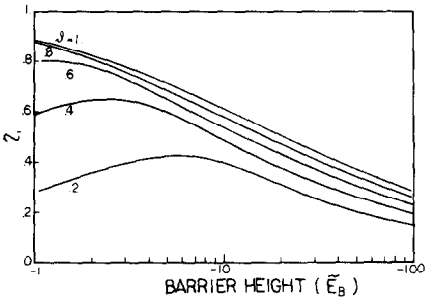

Fig. 4. The values of $\tilde{\eta}_1 = \eta$ are functions of the negative barrier height with the effective mass ratio ϑ. $\tilde{E}_B = E_B/kT$.

not lead to monotonic decrease of $\tilde{\eta}_1$. This is due to the mass deviation effect in which a quantity of $(1-1/\vartheta)E_\perp$ is added to the kinetic energy in the current flow direction. As the carrier reaches the second region, this additional kinetic energy effectively lowers the negative barrier which modifies η_1 as shown in Fig. 4. Both the QMT and $\tilde{\eta}_1$ are lowered although the magnitude of the barrier is smaller in the case of the lower barrier height. In fact, the current will be saturated classically when the barrier is negative. In this case, the series resistance becomes significant but we will not consider it here.

(b) *The* QMT *of carriers crossing a heterojunction*

Since the energy-band discontinuity exists in the interface of the heterojunction, carriers passing through the junction are reflected partly from the barrier. Similar to Schottky barrier, the quantum-mechanical reflection has to be taken into account to characterize the transport mechanism of heterojunctions. Especially, the QMT is an important factor when there is a large barrier in the junction or when the tunneling current has to be considered in heavily-doped materials.

In the calculation of the QMT, the WKB approximation is a powerful method and is applicable under the condition

$$\left|\frac{dk_x}{dx}\right| \ll k_x^2. \tag{29}$$

Let us consider the carrier flow shown in Fig. 5 where carriers transporting from left (side 1) to right (side 2). There is a depletion layer in side 1, but in side 2 there may be either depleted or accumulated region. Sometimes, surface charge is so large that both sides of the junction are accumulated; then the junction becomes an ohmic contact which is not interesting to us at present. In the depletion

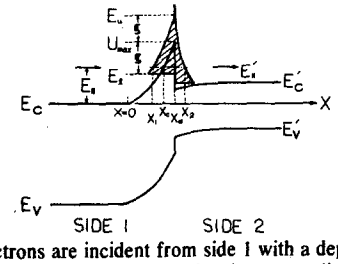

Fig. 5. Electrons are incident from side 1 with a depletion region to side 2. The KWB approximation is not applicable and the numerical solution is obtained in the shaded region.

region of side 1,

$$k_c = \frac{(2m^*)^{1/2}}{\hbar}(E_\parallel - U)^{1/2} \tag{30}$$

$$\frac{dk_x}{dx} = -\frac{m^*}{\hbar^2 k_x}\frac{dU}{dx} \tag{31}$$

$$\frac{dU}{dx} = \left[\frac{2q^2 N_N}{\epsilon} U\right]^{1/2} \tag{32}$$

where $E_\parallel$ = the parallel kinetic energy in the flat band region, U = the potential at x, N_N = the doping concentration of the semiconductor in side 1, ϵ = the dielectric constant of the semiconductor in side 1.

Substituting eqns (30)–(32) into eqn (29), the necessary condition of the WKB approximation becomes

$$E_{oo}^2 U \ll |E_\parallel - U|^3 \tag{33}$$

where $E_{oo} = \frac{q\hbar}{2}\left[\frac{N_N}{m^*\epsilon}\right]^{1/2}$. Let

$$\alpha = \left|\frac{dk_x}{dx}\Big/ k_x^2\right|,$$

then

$$E_{oo}^2 U = \alpha^2 (E_\parallel - U)^3. \tag{34}$$

The WKB approximation can be applied when α is much less than unity. Solving eqn (34), we obtain

$$E_u = U_{max} + \xi \tag{35}$$

$$E_l = U_{max} - \xi \tag{36}$$

where U_{max} = the peak potential energy with reference to E_C (see Fig. 5), $\xi = (E_{oo}^2 U_{max}/\alpha^2)^{1/3}$, E_u = the available lower bound of the WKB approximation when $E_\parallel > U_{max}$, E_l = the available upper bound of the WKB approximation when $E_\parallel < U_{max}$.

As $E_u > E_\parallel > E_l$, the WKB approximation is not accurate enough, and it will not be used to calculate the wave function of the entire depletion region. Solving eqn (34) for U in terms of $E_\parallel$ at the point $x = x_1$, we can get

$$U(x_1) = E_\parallel\left\{1 - \beta^{1/3}\left[\left(1 + \left(+\frac{8}{27}\beta\right)^{1/2}\right)^{1/3} + \left(1 - \left(1 + \frac{8}{27}\beta\right)^{1/2}\right)^{1/3}\right]\right\} \tag{37}$$

$$x_1 = \left[\frac{2\epsilon U(x_1)}{q^2 N_N}\right]^{1/2} \tag{38}$$

where

$$\beta = \frac{E_{oo}^2}{2\alpha^2 E_\parallel^2}.$$

In the region $0 < x < x_1$, the WKB approximation is sufficiently accurate. But the numerical calculation can not be avoided beyond this region, i.e. $x > x_1$. The momentum space is now divided into three parts by E_u and E_l, and the combined formulae using both the WKB approximation and the numerical method are derived as follows.

(i) $E_l < E_\parallel < E_u$

Because of the limitation of the WKB approximation, a closed form of the QMT cannot be found. Crowell and Sze [9] characterized the Schottky barrier by numerically solving the Schrodinger's equation. The method presented here modifies their work so that it can be used to characterize heterojunctions. Similarly to Crowell and Sze's treatment, we separate the junction into three parts at $x = x_1$ and $x = x_2$ between which the WKB approximation is inappropriate and Schrodinger's equation must be solved numerically. Let us assume ψ_1 and ψ_2 are two homogeneous solutions with the initial conditions.

$$\psi_1(x_1) = 1$$

$$\left.\frac{d\psi_1}{dx}\right|_{x=x_1} = 0$$

$$\psi_2(x_1) = 0$$

$$\left.\frac{d\psi_2}{dx}\right|_{x=x_1} = 1 \tag{39}$$

and the boundary conditions at $x = x_d$ (see Fig. 5) are

$$\psi_i(x_{d^+}) = \psi_i(x_{d^-})$$

$$\left.\frac{d\psi_i}{dx}\right|_{x=x_{d^+}} = \vartheta \left.\frac{d\psi_i}{dx}\right|_{x=x_{d^-}} \tag{40}$$

where $i = 1$ or 2. The total wave function ψ is a linear combination of ψ_1 and ψ_2

$$\psi = C\psi_1 + D\psi_2 \qquad \text{if } x_1 < x < x_2. \tag{41}$$

The WKB method gives the wave function in the regions $x < x_1$ and $x > x_2$ as

$$\psi = \frac{1}{k^{1/2}}[A\exp(i\gamma_I) + B\exp(-i\gamma_I)] \qquad \text{if } x < x_1 \tag{42}$$

$$\psi = \frac{E}{k^{1/2}}\exp(i\gamma_{II}) \qquad \text{if } x > x_2 \tag{43}$$

where $\gamma_I = \int_{x_1}^{x} k(x)\,dx$ and $\gamma_{II} = \int_{x_2}^{x} k(x)\,dx$. By matching the boundary conditions that the wave function and its derivative are continuous at $x = x_1$ and $x = x_2$, the QMT is found to be

$$T = \left\{\frac{1}{4k_1 k_2 \vartheta}[(\zeta_1 - \zeta_3\theta_0)^2 + (\zeta_2 - \zeta_4\theta_0)^2 + k_1^2(\zeta_3^2 + \zeta_4^2)] + \frac{1}{2}\right\}^{-1} \tag{44}$$

where

$$\zeta_1 = \left.\frac{d\psi_1}{dx}\right|_{x=x_2} + \frac{1}{2k_2}\frac{dk_2}{dx}\psi_1(x_2)$$

$$\zeta_2 = k_2\psi_1(x_2)$$

$$\zeta_3 = \left.\frac{d\psi_2}{dx}\right|_{x=x_2} + \frac{1}{2k_2}\frac{dk_2}{dx}\psi_2(x_2)$$

$$\zeta_4 = k_2\psi_2(x_2)$$
$$\theta_0 = \frac{1}{2k_1}\frac{dk_1}{dx}\bigg|_{x=x_1}. \tag{45}$$

All ζ's and k_2, (dk_2/dx) are values at $x = x_2$ where the WKB approximation is again valid. k_1 and (dk_1/dx) are values at $x = x_1$. Here, we have also used condition[9]

$$\psi_1(x_2)\frac{d\psi_2}{dx}\bigg|_{x=x_2} - \psi_2(x_2)\frac{d\psi_1}{dx}\bigg|_{x=x_2}$$
$$= \vartheta\left[\psi_1(x_1)\frac{d\psi_2}{dx}\bigg|_{x=x_1} - \psi_2(x_1)\frac{d\psi_1}{dx}\bigg|_{x=x_1}\right] \tag{46}$$
$$= \vartheta$$

which can be obtained from the current flow formula.

(ii) $E_\parallel > E_u$

From the definition of E_u, the WKB approximation can be used in the entire depletion region of side 1. Equation (44) is also applicable in this case, if we let $x_1 = x_{d^-}$ so that we can use the same program to calculate the QMT's in cases (i) and (ii). When the barrier is a step function, $(dk_1/dx) = 0$, $(dk_2/dx) = 0$, $\zeta_1 = \zeta_4 = \theta_0 = 0$, $\zeta_2 = k_2$ and $\zeta_3 = \vartheta$ and it is found that eqn (44) is reduced to eqn (25) for the ideal case.

(iii) $E_\parallel < E_1$

When the parallel kinetic energy is less than E_u, the WKB approximation can be used from $x = 0$ to $x = x_d$ and the numerical wave functions are used in side 2 as in case (i). The QMT is given by

$$T = \left\{\frac{1}{4\kappa_1 k_2 \vartheta}\left[\frac{\lambda^2}{4}((\zeta_1 - \zeta_3\theta_1)^2 + (\zeta_2 - \zeta_4\theta_1)^2)\right.\right.$$
$$\left.\left. + \lambda^{-2}((\zeta_1 - \zeta_3\theta_2)^2 + (\zeta_2 - \zeta_4\theta_2)^2)\right] + \frac{1}{2}\right\}^{-1} \tag{47}$$

$$\lambda = \exp\left[-\int_{x_c}^{x_d}\kappa_x(x')\,dx'\right]. \tag{48}$$

where all ζ's are the same as eqn (45) and

$$\theta_1 = \frac{1}{2\kappa_1}\frac{d\kappa_1}{dx} + \kappa_1$$
$$\theta_2 = \frac{1}{2\kappa_1}\frac{d\kappa_1}{dx} - \kappa_1 \tag{49}$$

κ_1 is the imaginary wave number at $x_1 = x_d$, and $(d\kappa_1/dx)$ is its derivative, $x_c = x_d(E_\parallel/\cup_{max})^{1/2}$.

4. APPLICATION TO THE *N-n* HETEROJUNCTION

The general theory of carrier transport across the heterojunction has been presented in the previous sections. In this section, the *N-n* heterojunction with different effective masses on both sides and the energy-band discontinuity at the interface will be used as an example to explain the above model for calculating the I-V characteristics. Although Chang[21] has made use of the thermionic emission to model the Ge-$GaAs_{1-x}P_x$ *N-n* junction in low voltages, the analytical form is available only for a limited range of doping. According to the analysis of Crowell *et al.*[20], the tunneling current is not negligible, especially, when the energy-band discontinuity or the doping is high. Therefore, the T-F model must be employed in the general case. The band structure of an abrupt *N-n* junction under the bias V_{BS} is shown in Fig. 6. The forward bias is defined as the positive voltage V_{BS} applied to the side of the small energy band. Then, the surface potential ϕ_1 of side 1 is given by

$$\phi_1 = -\frac{qN_N x_d^2}{2\epsilon_N}$$
$$= -\frac{\epsilon_N \mathscr{F}_{max}}{2qN_N}, \tag{50}$$

where N_N is the donor density, x_d is the depletion width of the depletion region and ϵ_N is the dielectric constant of the larger-energy-band-gap semiconductor in side 1. $\mathscr{F}_{max}$ is the maximum electric field at the interface. It can also be expressed in terms of the parameters of the semiconductor in side 2. Using Poisson's equation, the potential $\phi(x)$ in side 2 is given by

$$\frac{d^2\phi(x)}{dx^2} = \frac{-q}{\epsilon_n}[N_{Dn}^+ - N_{An}^- + p - n]$$
$$= \frac{-q}{\epsilon_n}\left[N_{Dn}\frac{1}{1 + g_e\exp\left(\frac{q\phi(x) + E_{fn} + E_d}{kT}\right)}\right.$$
$$- N_{An}\frac{1}{1 + g_h^{-1}\exp\left(\frac{-q\phi(x) + E_{fp} + E_a}{kT}\right)}$$
$$+ N_{Vn}\frac{2}{\sqrt{\pi}}\mathscr{F}^{1/2}\left(\frac{-q\phi(x) + E_{fp}}{kT}\right)$$
$$\left. - N_{Cn}\frac{2}{\sqrt{\pi}}\mathscr{F}^{1/2}\left(\frac{q\phi(x) + E_{fn}}{kT}\right)\right] \tag{51}$$

where ϵ_n is the dielectric constant of the semiconductor in side 2, N_{Dn} and N_{An} are the densities of donor and acceptor, E_d and E_a are the ionization energy for electron and hole, E_{fn} and E_{fp} are electron and hole quasi-Fermi levels referred to the corresponding energy-band edges, g_e and g_h are degeneracy factors of electron and hole, N_{Cn} and N_{Vn} are the effective density states in the conduction band and the valence band, respectively. $\mathscr{F}^{1/2}$ is the Fermi-Dirac integral. Assuming constant quasi-Fermi levels, we multiply $d\phi(x)$ on both sides of eqn (51)

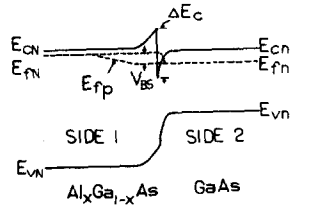

Fig. 6. The band diagram of the *N-n* heterojunction under the bias V_{BS}.

and integrate the right-hand side from $\phi(\infty) = 0$ to $\phi(0) = \phi_2$ and the left-hand side from $(d\phi/dx)|_{x=\infty} = 0$ to $(d\phi/dx)|_{x=0} = -\mathcal{F}_{max}$. Then, we obtain

$$\mathcal{F}_{max}^2 = \frac{2kT}{\epsilon_n}\left\{N_{Dn}\ln\left[\frac{\exp\left(-\frac{q\phi_2}{kT}\right)+g_e\exp\left(\frac{E_{fn}+E_d}{kT}\right)}{1+g_e\exp\left(\frac{E_{fn}+E_d}{kT}\right)}\right]\right.$$
$$+N_{An}\ln\left[\frac{\exp\left(\frac{q\phi_2}{kT}\right)+g_h^{-1}\exp\left(\frac{E_{fp}+E_a}{kT}\right)}{1+g_h^{-1}\exp\left(\frac{E_{fp}+E_a}{kT}\right)}\right]$$
$$+N_{Vn}\frac{2}{\sqrt{\pi}}\left[G\left(\frac{E_{fp}-q\phi_2}{kT}\right)-G\left(\frac{E_{fp}}{kT}\right)\right]$$
$$\left.+N_{Cn}\frac{2}{\sqrt{\pi}}\left[G\left(\frac{E_{fn}+q\phi_2}{kT}\right)-G\left(\frac{E_{fn}}{kT}\right)\right]\right\} \quad (52)$$

where $G(x) = \int_{-\infty}^{x}\mathcal{F}^{1/2}(x')\,dx'$.

From the band diagram shown in Fig. 6 we get

$$qV_{BS} = E_{fN} - E_{fn} + q\phi_1 - q\phi_2 + \Delta E_c. \quad (53)$$

By making use of eqns (50)–(53), the self-consistent solutions of ϕ_1 and ϕ_2 can be obtained for a given bias V_{BS}. Therefore, the band bending of the junction is determined and the QMT of the carrier passing through the potential barrier of this bending can be calculated. Substituting the QMT into eqn (10), the current-voltage relationship can be found by the numerical integration.

The $Al_xGa_{1-x}As$-GaAs heterojunction is employed in the DH laser structures [23]. Our study of the $Al_xGa_{1-x}As$-GaAs N-n junction is intended to help understand the current transport mechanism in these lasers. We have made use of the parameters of $Al_xGa_{1-x}As$ collected by Rode [22] and calculated the I-V characteristics of $Al_xGa_{1-x}As$-GaAs N-n junction. The results are shown in Figs. 7 and 8. Note that the rectifying characteristics are obtained, but the reverse current is not saturated. The current increases with the doping concentration of $Al_xGa_{1-x}As$ similar to a Schottky diode when we treat the accumulated GaAs as a metal. The larger the x-value and the conduction-band discontinuity, $\Delta E_C = 0.85\,\Delta E_g$ [24], the lower the current passing through the junction.

Let us neglect the tunneling effect and quantum-mechanical reflection. We set the transmission coefficient T to one for carriers with a kinetic energy greater than the barrier height and to zero, otherwise, the current density of this classical consideration becomes

$$J = A^*T^2\exp\left[\frac{E_{fN}-q\phi_1}{kT}\right]\left[1-\exp\left(-\frac{qV_{BS}}{kT}\right)\right]$$
$$= A^{*\prime}T^2\exp\left[\frac{E_{fn}+q\phi_2-\Delta E_c}{kT}\right]\left[\exp\left(\frac{qV_{BS}}{kT}\right)-1\right] \quad (54)$$

where we use the condition that the mass ratio ϑ is near unity. Comparing this classical form of the thermionic emission to the exact current density in the case of the doping density of 10^{17} cm^{-3} in $Al_xGa_{1-x}As$ and 10^{15} cm^{-3} in GaAs, we find that the classical approximation is about one half of the exact value at low voltage because the tunneling current has not been included [19]. The effect of quantum-mechanical reflection is also shown in the higher bias where the result of the classical approximation is larger than the more exact value. These discrepancies are shown in Fig. 9. The larger ideality factor obtained exhibits the quantum-mechanical effect based on the transport theory presented here. Of course, the series resistance is also a factor that increases the n-value in the real diode characteristics.

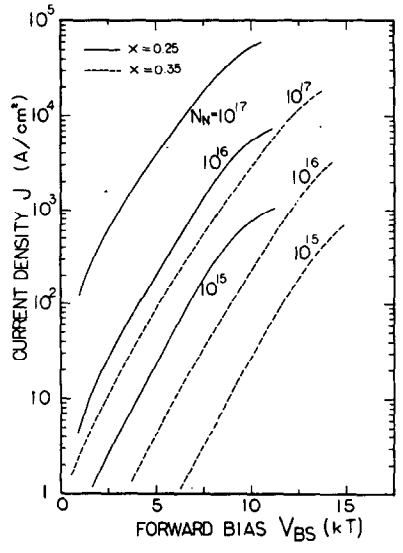

Fig. 7. The forward current of the N-n $Al_xGa_{1-x}As$-GaAs junction under the bias V_{BS}, Nn is the doping of the ternary compound and that of GaAs is 10^{15} cm^{-3}.

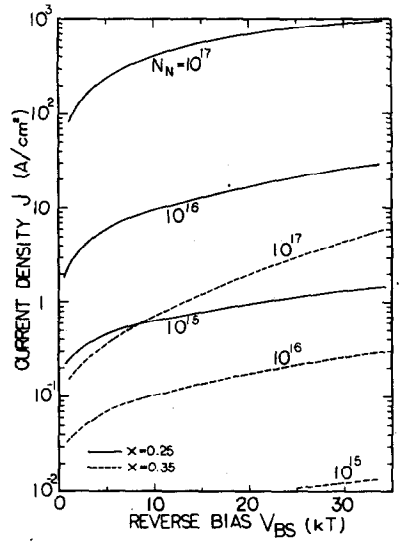

Fig. 8. The reverse current of the N-n $Al_xGa_{1-x}As$-GaAs junction under the bias V_{BS}, Nn is the doping of the ternary compound and that of GaAs is 10^{15} cm^{-3}.

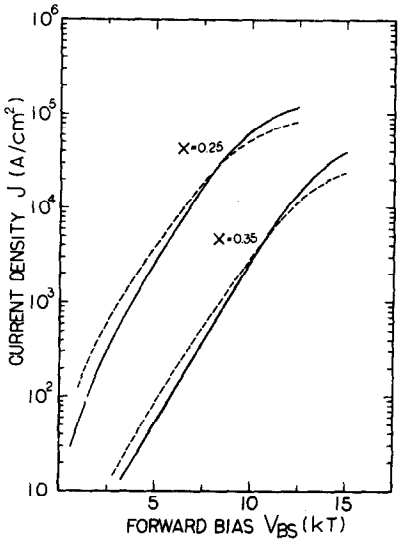

Fig. 9. The forward current of the N-n junction calculated by (a) the quantum mechanical reflection T-F model with the dash line (b) the classical thermionic emission model with the solid line. The dopant density of $Al_xGa_{1-x}As$ is 10^{17} cm^{-3} and that of GaAs is 10^{15} cm^{-3}.

5. CONCLUSIONS

The transport equations are examined in the heterojunction interface, especially concerned with the different masses of carriers in both sides of either an isotype or anisotype heterojunction. The upper and lower limits of the perpendicular component of the kinetic energy are, in general, not infinity and zero, respectively. The general form of the current density is derived as given in eqn (18) by assuming an isotropic effective mass. In the model presented in this paper, the perpendicular component of the kinetic energy is modified by $1/\vartheta$ so that the perpendicular momentum is conserved when carriers pass through the barrier. For the conservation of the total energy, this modulated perpendicular kinetic energy of $(1/\vartheta - 1)E_\perp$ plays a role in reducing effectively the barrier height in the calculation of the quantum-mechanical transmission coefficient. Since the WKB approximation cannot be used to calculate the quantum-mechanical transmission when the kinetic energy is around the peak of the potential barrier, we have used a combined WKB-numerical method in which the parallel kinetic energy is considered separately in three regions: (i) $E_\parallel > E_u$ in which the WKB method is valid, (ii) $E_u > E_\parallel > E_l$ in which the numerical method is used, and (iii) $E_\parallel < E_l$ in which the WKB method is employed in the depletion region of side 1 and the numerical method is used in side 2. Referring Rode's work[22] on AlGaAs-GaAs DH laser, Al_xGa_{1-x} As-GaAs N-n junction is taken as an example to calculate the current densities under both forward and reverse biasing voltages. At high biasing, the forward characteristics show that the quantum-mechanical reflection reduces the current density to sixty per cent of its classical value. But at low biasing, it shows that the tunneling current must be considered as the semiconductor of the larger energy-band gap is heavily doped. This transport theory is applicable to the anisotype heterojunction. However, we must take into account the diffusion mechanism in series with the T-F emission considered in this paper.

Acknowledgement—The authors would like to thank the reviewers who make valuable suggestions as well as technical corrections.

REFERENCES

1. W. Shockley, *Bell Syst. Tech. J.* **28**, 435 (1949).
2. W. Schottky, *Natarwiss.* **26**, 843 (1938).
3. H. A. Bethe, MIT Radiation Laboratory, Report 43–12 (1942).
4. E. O. Kane, *J. Appl. Phys.* **32**, 83 (1961).
5. W. A. Harrison, *Phys. Rev.* **123**, 85 (1961).
6. R. Stratton, *Phys. Rev.* **125**, 67 (1962).
7. C. R. Crowell, *Solid-St. Electron.* **8**, 395 (1965).
8. C. R. Crowell and S. M. Sze, *Solid-St. Electron.* **9**, 1035 (1966).
9. C. R. Crowell and S. M. Sze, *J. Appl. Phys.* **37**, 2683 (1966).
10. R. L. Anderson, *Solid-St. Electron.* **5**, 341 (1962).
11. R. H. Rediker, S. Stopek and J. H. R. Ward, *Solid-St. Electron.* **7**, 621 (1964).
12. V. Dolega, *Z. Natarforsch*, **18**, 653 (1963).
13. L. J. van Ruyven, J. M. P. Papenhuijzen and A. C. J. Verhoeven, *Solid-St. Electron.* **8**, 631 (1965).
14. S. S. Perlman and D. L. Feucht, *Solid-St. Electron.* **7**, 911 (1964).
15. A. R. Riben and D. L. Feucht, *Int. J. Electron.* **20**, 583 (1966).
16. J. P. Donnelly and A. G. Milnes, *Proc. IEEE* **113**, 1468 (1966).
17. A. G. Milnes and D. L. Feucht, *Heterojunctions and M-S Junctions.* Academic Press, New York (1972).
18. H. C. Casey and M. B. Panish, *Heterostructure Lasers, Part A: Fundamental Principles*, Chap. 4 (1978).
19. T. L. Tansley and S. J. T. Owen, *IEEE Trans. Electron. Dev.* **ED-23**, 1123 (1976).
20. C. R. Crowell and V. L. Rideout, *Solid-St. Electron.* **12**, 89 (1969).
21. L. L. Chang, *Solid-St. Electron.* **8**, 721 (1965).
22. D. L. Rode, *J. Appl. Phys.* **45**, 3887 (1974).
23. M. B. Panish, *Proc. IEEE* **64**, 1512 (1976).
24. R. Dingle, W. Wigmann and C. H. Henry, *Phys. Rev. Lett.* **33**, 827 (1974).